Original Article

Cephalalgia
An International Journal of Headache

International Headache Society

Fluorescently-labeled fremanezumab is distributed to sensory and autonomic ganglia and the dura but not to the brain of rats with uncompromised blood brain barrier

Cephalalgia
40(3) 229–240

Article reuse guidelines:
sagepub.com/journals-permissions
DOI: 10.1177/0333102419896760
journals.sagepub.com/home/cep

Rodrigo Noseda[1,2], Aaron J Schain[1,2], Agustin Melo-Carrillo[1,2], Jason Tien[3], Jennifer Stratton[3], Fanny Mai[1], Andrew M Strassman[1,2] and Rami Burstein[1,2]

Abstract

Background: The presence of calcitonin gene-related peptide and its receptors in multiple brain areas and peripheral tissues previously implicated in migraine initiation and its many associated symptoms raises the possibility that humanized monoclonal anti-calcitonin gene-related peptide antibodies (CGRP-mAbs) can prevent migraine by modulating neuronal behavior inside and outside the brain. Critical to our ability to conduct a fair discussion over the mechanisms of action of CGRP-mAbs in migraine prevention is data generation that determines which of the many possible peripheral and central sites are accessible to these antibodies – a question raised frequently due to their large size.

Material and methods: Rats with uncompromised and compromised blood-brain barrier (BBB) were injected with Alexa Fluor 594-conjugated fremanezumab (Frema594), sacrificed 4 h or 7 d later, and relevant tissues were examined for the presence of Frema594.

Results: In rats with uncompromised BBB, Frema594 was similarly observed at 4 h and 7 d in the dura, dural blood vessels, trigeminal ganglion, C2 dorsal root ganglion, the parasympathetic sphenopalatine ganglion and the sympathetic superior cervical ganglion but not in the spinal trigeminal nucleus, thalamus, hypothalamus or cortex. In rats with compromised BBB, Frema594 was detected in the cortex (100 μm surrounding the compromised BBB site) 4 h but not 7 d after injections.

Discussion: Our inability to detect fluorescent (CGRP-mAbs) in the brain supports the conclusion that CGRP-mAbs prevent the headache phase of migraine by acting mostly, if not exclusively, outside the brain as the amount of CGRP-mAbs that enters the brain (if any) is too small to be physiologically meaningful.

Keywords

Migraine, headache, CGRP, monoclonal antibodies, trigeminovascular, CSD

Date received: 12 November 2019; revised: 26 November 2019; 2 December 2019; accepted: 3 December 2019

Introduction

The view that calcitonin gene-related peptide (CGRP) plays a role in migraine pathophysiology is supported by data that demonstrate its ability to trigger a migraine-like headache when infused intravenously (1), its increased level in the jugular vein during the ictal phase of spontaneous migraine attacks (2), its presence in meningeal nociceptors (3,4), and studies demonstrating photophobic behavior in mice genetically modified to express increased CGRP receptors (5).

[1]Department of Anesthesia, Critical Care and Pain Medicine, Beth Israel Deaconess Medical Center, Boston MA, USA
[2]Harvard Medical School, Boston, MA, USA
[3]Teva Biologics, Redwood City, CA, USA

Corresponding author:
Rami Burstein, CLS-649, 3 Blackfan Circle, Boston, MA 02215, USA.
Email: rburstei@bidmc.harvard.edu

Because CGRP and CGRP receptors are found both outside (6–8) and inside (9–11) the central nervous system and near meningeal and cerebrovascular blood vessels (12), it is likely that CGRP's role in the many facets of migraine pathophysiology is mediated in part by its ability to dilate relevant blood vessels, as well as by its ability to modulate the behavior of nociceptive neurons in the periphery (i.e. meningeal nociceptors) and neurons in the cortex, hippocampus, hypothalamus, thalamus, amygdala, septum, cerebellum, periaqueductal gray, locus coeruleus, nucleus raphe magnus (10,11) – all areas that contain neurons that regulate sensory, autonomic, endocrine, cognitive and affective functions in brain areas believed to play a role in the production of many of the classical migraine-associated symptoms (10,13).

The wide distribution of CGRP and its receptors along the trigeminovascular pathway (i.e. trigeminal ganglion, spinal trigeminal nucleus, and thalamus (10)) and the many brain areas that receive trigeminovascular input (i.e. multiple brainstem, hypothalamic, subcortical and cortical nuclei and regions (10,11)), raise the possibility that humanized monoclonal anti-CGRP antibodies and anti-CGRP receptors antibodies, which are effective migraine preventives (14–17), can interfere with peripheral and central mechanisms that facilitate the initiation of migraine attacks and the associated headaches. Critical to our ability to conduct a fair discussion over the mechanisms of action of this class of drugs in migraine prevention is the generation of data that determine which of the many possible peripheral and central sites (nuclei, organs, structures) are accessible to anti-CGRP and anti-CGRP receptors antibodies – a question raised frequently due to their large size (about 150,000 Dalton).

Material and methods

Animals: Sixteen male Sprague-Dawley rats weighting 250–350 g (for histology) were used in this study. Experiments were conducted in accordance with NIH guidelines and approved by the Institutional Animal Care and Use Committee at Harvard Medical School and Beth Israel Deaconess Medical Center. Animals were housed in a controlled environment (22°C RT; 12 h light/dark cycle) with free access to food and water.

Monoclonal antibody against CGRP: Alexa Fluor 594-conjugated fremanezumab (Frema594) was obtained from Teva Pharmaceuticals (Petah Tikva, Israel), and injected at 30 mg/kg. Fremanezumab was conjugated via reaction with a succinimidyl ester of Alexa Fluor 594 (ThermoFisher #A20004) in PBS, pH 9.0, mixing in a 1:2 antibody to dye molar ratio for 4 h at room temperature. Unreacted dye was removed by size exclusion chromatography through a Zeba desalting column (ThermoFisher #89891).

Intravenous injections of Alexa Fluor 594-conjugated fremanezumab: Rats were placed in an induction chamber connected to a gas anesthesia machine delivering 5% isoflurane in O_2 (200 ml/min). After induction, animals were switched to a nosecone or intubated to receive 2% isoflurane until the end of the procedure. Rats were placed on a homeothermic blanket; heart rate, blood oxygen saturation and body temperature were continuously monitored. A plastic bag with warm water (40°C) was placed on the tail for about 10 min to induce local vasodilation. A 24 G intravenous catheter was introduced into the left lateral tail vein until blood was visible, and then connected to a 1 ml syringe. These experiments were conducted in one group of rats in which the blood-brain barrier (BBB) was not disrupted (group 1) and a second group in which the BBB was disrupted locally (group 2) . In group 1 (n = 8), a single bolus of Alexa Fluor 594-conjugated fremanezumab (30 mg/kg) or NaCl 0.9% was injected in naïve rats (i.e. rats not exposed to craniotomy or cortical spreading depression). In this group, rats were allowed to recover from gas anesthesia and then placed in their cages for 4 h (n = 3) or 1 week (n = 3) after Frema594 or saline injections (n = 2). In group 2 (n = 8), the BBB was disrupted mechanically by the insertion of a glass recording electrode in the visual cortex and a stainless-steel electrode (commonly used to induce CSD) in the frontal cortex (as described in detail in our recent papers (18,19). We chose this method in order to produce a localized area of BBB disruption, instead of the global disruption caused by systemic administration of chemical or hyperosmotic agents. We found this to be advantageous in allowing visual comparison of the level of fluorescence in the disrupted region versus undamaged regions within the same animal (in addition to our comparison between saline-treated and Frema594-treated animals). Frema594 (30 mg/kg) was injected immediately after insertion of the recording electrode in the visual cortex, but 4 h before insertion of the stainless-steel electrode in the frontal cortex. Four hours after injections, rats (n = 3 Frema594; n = 1 saline) were euthanized with an overdose of Pentobarbital (150 mg/kg, i.p.). Rats allowed to survive for 1 week (n = 3 Frema594; n = 1 saline), were sutured, disinfected, provided with painkillers (Meloxicam SR 4 mg/kg s.c.), placed in their cages, and monitored daily for discomfort or stress as determined by proper grooming, food consumption and social interactions, until euthanasia.

Tissue collection and processing: After the corresponding survival period, rats were deeply anesthetized with an overdose of pentobarbital sodium (150 mg/kg,

i.p.) and perfused with 200 ml heparinized saline followed by a fixative solution containing 400 ml of paraformaldehyde (4%) and 20 ml of picric acid (1.3%) in 0.1 M phosphate buffered saline (PBS). We then collected all relevant peripheral tissue including large areas of the dura, trigeminal ganglion (TG), C2 dorsal root ganglion (C2 DRG), sphenopalatine ganglion (SPG), superior cervical ganglion (SCG), as well as the whole brain and upper cervical spinal cord. The dura was flat mounted on slide with Vectashield mounting medium (Vector), coverslipped and stored for 2 h in the dark before imaging. All other tissues were cryoprotected in 30% sucrose PBS for 48 h, frozen and cut into serial sections (20–40 μm thick) using a cryostat (Leica CM3050S). TG, C2 DRG SPG and SCG sections were thaw-mounted directly onto slides, coverslipped with mounting media and stored for 2 h in the dark before imaging. Sections of brain tissue were collected in PBS, mounted on slide, coverslipped with mounting media and stored for 2 h in the dark before imaging.

Digital imaging of peripheral and central tissues: Digital imaging of labeling in the dura, TG, C2 DRG, SPG, SCG, brain areas and SpV was performed on a fluorescence scanning microscope (Leica DM5500) that compiled 1–1.5 μm-thick scans using a z-stacking software application (LASX, Leica). Labeling of Alexa Fluor 594-conjugated fremanezumab was detected by excitation/emission at 551/624 nm (red). Microscope settings for image acquisition were identical for all red images (exposure = 300 ms; gamma = 1; gain = 1). No shading or brightness correction was used. Additional images for visualization of structures and as control images were acquired by excitation/emission at 455/520 nm (green) and 358/461 nm (blue) respectively. Photomicrographs of double/triple-labeling were obtained by superimposition of green, red and blue images.

Results

Uncompromised (intact) blood-brain barrier

In naïve rats, intravenous infusion of fluorescently conjugated fremanezumab produced intense labeling in the dura, dural blood vessels, trigeminal ganglion, C2 dorsal root ganglion, the parasympathetic sphenopalatine ganglion and the sympathetic superior cervical ganglion but not in the spinal trigeminal nucleus, thalamus, hypothalamus or cortex.

Dura: In saline-treated rats, no fluorescent signal was detected in the dura (Figure 1(a)–(b)), while in Frema594-treated rats, fluorescent signal was readily detected throughout the dura, including the transverse sinus, and in blood vessel walls (Figure1(c)–(d)), and occasionally in axonal fibers (Figure 1(c), middle, right). The distribution of Frema594 in the dura appeared similar 4 hours (as in Schain et al. (20)) and 1 week after it was injected intravenously.

Sensory ganglia: In saline-treated rats, no fluorescent signal was detected in the trigeminal ganglion or C2 DRG (Figure 2(a)), while in Frema594 treated rats, fluorescent signal was readily detected in extracellular spaces surrounding sensory cell somas, blood vessels walls, and perineural tissue (Figure 2(b)–(c)). The distribution of Frema594 in these sensory ganglia appeared to be similar 4 h and 1 week after it was injected intravenously.

Autonomic ganglia: In saline-treated rats, no fluorescent signal was detected in the SPG or SCG (Figure 3(a)), while in Frema594-treated rats, fluorescent signal was detectable in extracellular spaces that surround autonomic cell somas, and highly present within blood vessels walls and perineural tissue (Figure 3(b)). The distribution of Frema594 in these sensory ganglia appeared similar 4 h (data not shown) and 1 week (Figure 3(b)) after it was injected intravenously.

Central nervous system: Unlike in the periphery, at no time after treatment with saline or Frema594 (i.e. 4 h and 1 week), were we able to detect fluorescent labeling in the spinal trigeminal nucleus (Figure 4(a)), cerebral cortex (Figure 4(b)), hypothalamus (Figure 4(c)) or thalamus (Figure 4(d)) of any rat.

Locally compromised blood-brain barrier. In rats in which a recording electrode and pinprick needle were inserted into the cortex through the dura and pia, intravenous infusion of fluorescently conjugated fremanezumab produced similar labeling in the dura, dural blood vessels, trigeminal ganglion, C2 dorsal root ganglion, the parasympathetic sphenopalatine ganglion and the sympathetic superior cervical ganglion (data not shown) and in a restricted (approximately 100 μm) area in the cortex surrounding the tip of the recording electrode or the pinprick needle.

Cerebral cortex: Four hours after injection of Frema594, fluorescent labeling was detected along the track of the recording electrode, whereas in the cortex itself labeling was seen as far as 100 μm from the track itself (Figure 5(b)); in the pia it was detected as far as 1 mm from the electrode penetration site (Figure 5 (b)–(d)). As shown in Figure 5(e), fluorescent labeling was also detected in the cortical area surrounding the manual penetration of the pinprick needle and the pia above it. In spite of the presence of Frema594 along the area where the BBB was broken, we were unable to detect any fluorescent signal in any region of the contralateral cortex or the pia above it. Unexpectedly, in cortical areas where the recording electrode did not cause lesion, Frema594 was not visible a week after it

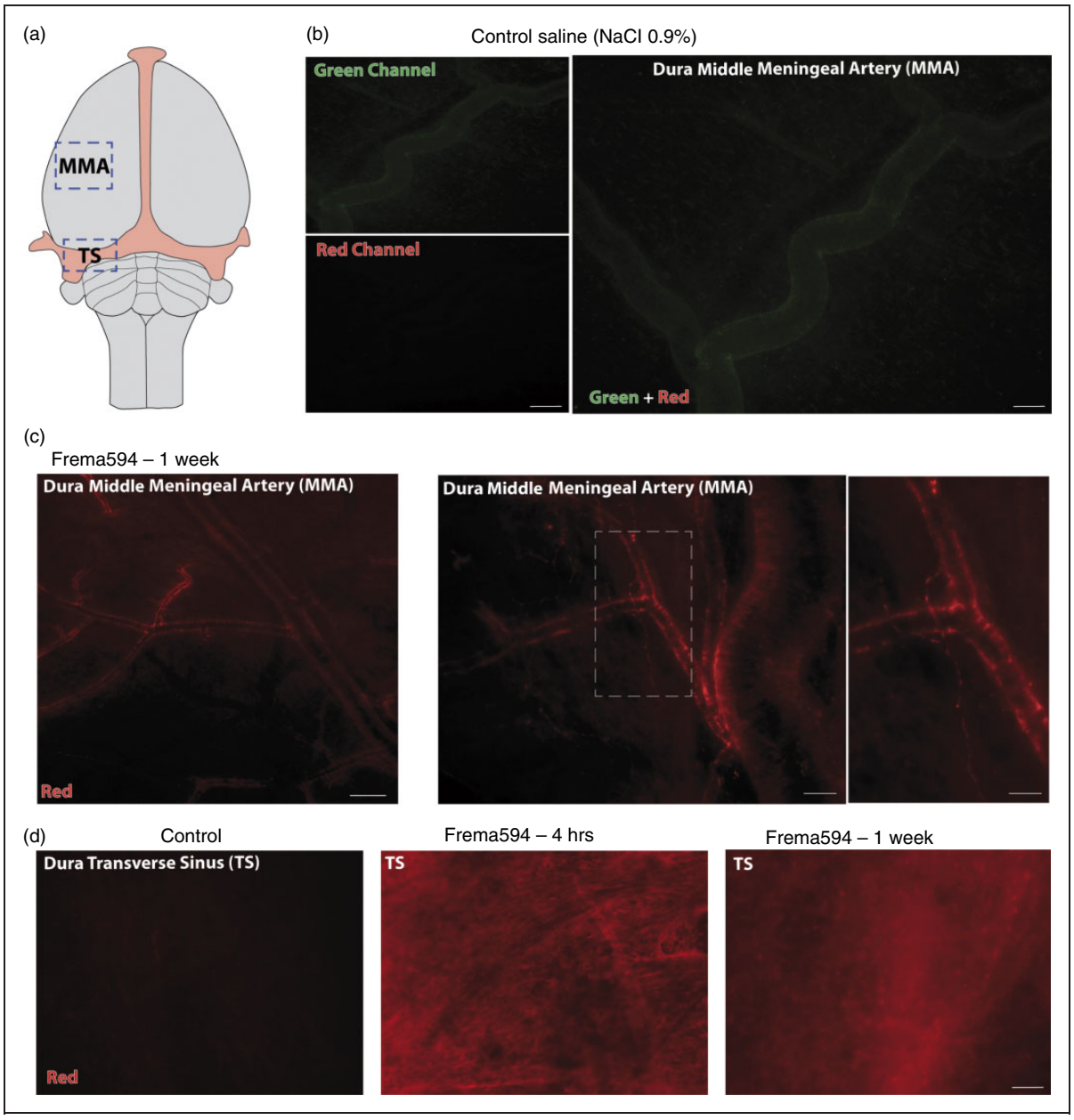

Figure 1. Imaging Frema594 in whole-mount dura after i.v. injection of Frema594 or saline. (a) Schematic overview of the rat brain depicting areas of the overlying dura shown in Figures (b)–(d). (b) Saline injections induce no detectable fluorescent signal in the dura overlying the middle meningeal artery (MMA). (c) In the same area, distinct Frema594 labeling is seen in blood vessel walls (left) and axons (middle, right) 1 week after injection was made. (d) In the dura overlying the transverse sinus (TS), Frema594 labeling is seen throughout the dura at 4 hours and 1 week after injection (middle, right) but not after saline control (left). Green channel is shown for visualization of autofluorescence at 455/520 nm of unlabeled structures as an anatomical reference. Red channel shows Frema594 fluorescent signal at 551/624 nm. Scale bar = 100 μm.

was detected in this same area (Figure 6(a)–(b)). In contrast, in the cortical area where the manual insertion of the CSD electrode caused a small lesion (Figure 6(c)), Frema594 was visible in several axons near the lesion site and in the pia just above it (Figure 6(d)) – raising the possibility that CGRP-mAbs may be able to reach brain parenchyma surrounding lesions.

Discussion

In rats with intact BBB, intravenous infusion of fluorescently conjugated fremanezumab produced intense labeling in the dura, dural and pial blood vessels, trigeminal ganglion, C2 dorsal root ganglion, the parasympathetic sphenopalatine ganglion and the

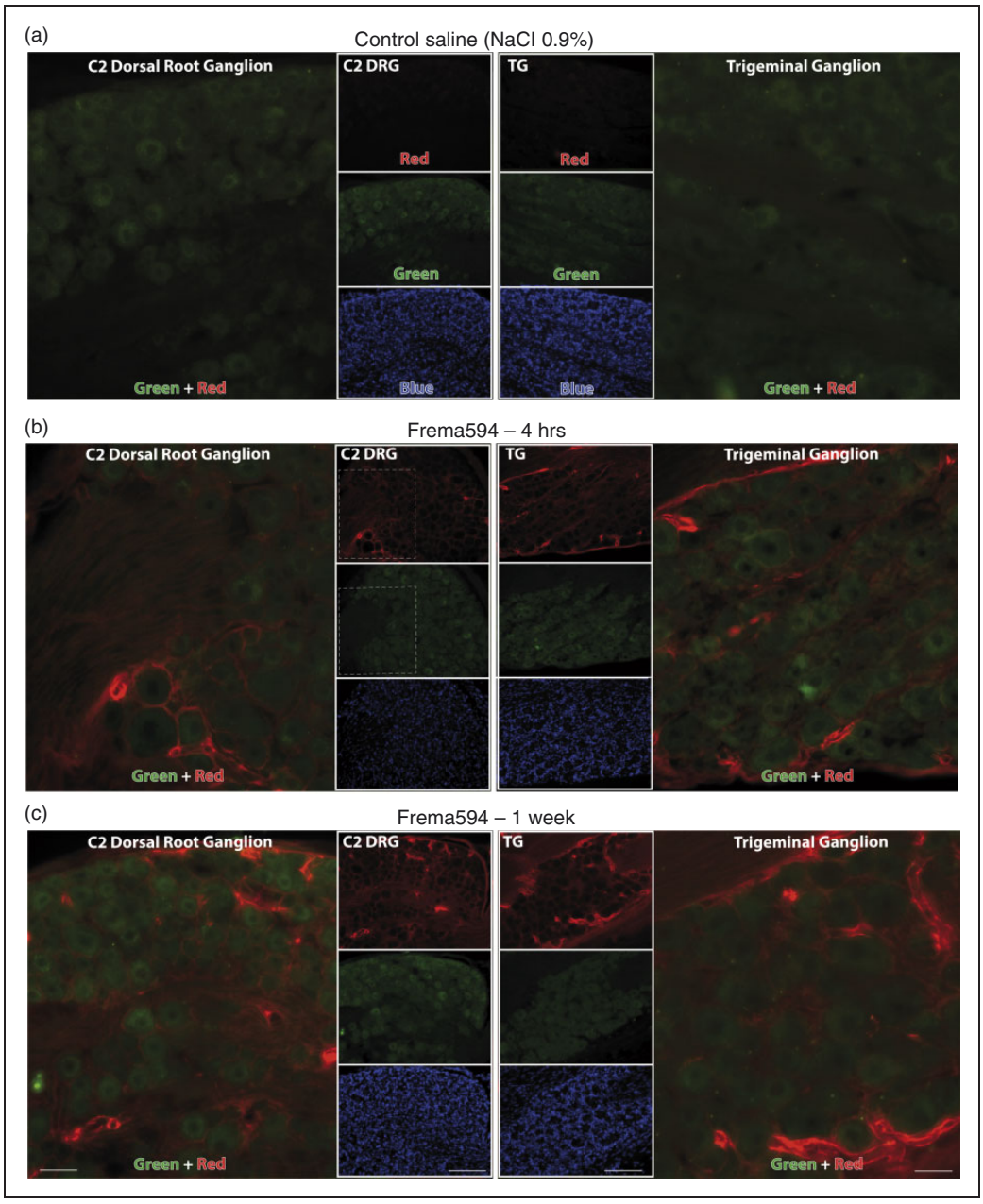

Figure 2. Imaging Frema594 in C2 dorsal root ganglion and the trigeminal ganglion. (a) Saline injections produce no fluorescent labeling in sensory ganglia. (b)–(c) Frema594 injections produce selective (red only) labeling in extracellular spaces surrounding cell somas, blood vessel walls and perineural tissue that envelops both C2 and the trigeminal ganglia. The fluorescent labeling appears similar at 4 hours and 1 week after injections. Blue channel shows nuclear staining with DAPI. Scale bar = 100 μm.

sympathetic superior cervical ganglion. In contrast no detectable level of the fluorescently labeled fremanezumab was seen in the spinal trigeminal nucleus, thalamus, hypothalamus or cortex. Our inability to detect any fluorescent (CGRP-mAbs) signal in the brain supports the conclusion that CGRP-mAbs prevent the headache phase of migraine by acting mostly, if not exclusively, outside the brain as the amount of CGRP-mAbs that enters the brain (if any) may not be sufficient to alter neuronal behavior.

It may be interesting to note that in both sensory and autonomic ganglia, Frema594 was visualized in the space surrounding each individual neuron but not inside the sensory or autonomic neurons themselves. The space surrounding each ganglion neuron is bounded by a ring of satellite glial cells (SGCs), which control the microenvironment of the neurons they envelop (21,22). Recent studies have described CGRP receptors on SGCs (7,23), which suggests that CGRP can be released into this extracellular space.

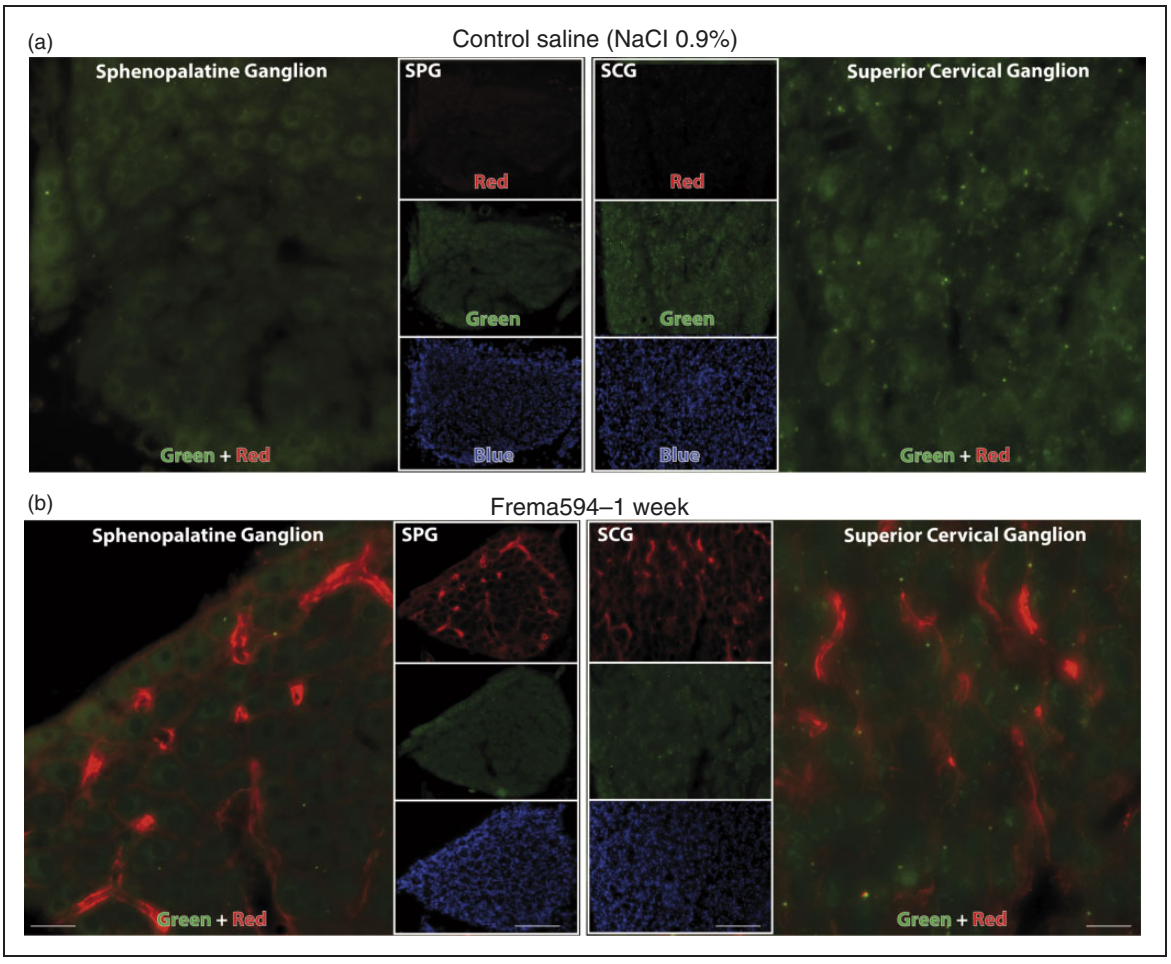

Figure 3. Imaging Frema594 in the sphenopalatine and superior cervical ganglia. (a) Saline injections produce no fluorescent labeling in these autonomic ganglia. (b) At 1 week post injections, Frema594 produce selective (red only) labeling in extracellular spaces surrounding cell somas, blood vessel walls and perineural tissue that envelops these ganglia. Scale bar = 100 μm.

Our finding of Frema594 in this space would be consistent with this possibility, as the Frema594 would be expected to bind to the CGRP.

The presence of Frema594 in the dura, trigeminal, and upper cervical sensory ganglia supports the view that CGRP-mAbs can prevent the headache phase of migraine by blocking CGRP-dependent functions in these organs (18,24). Frema594 presence in the sphenopalatine and superior cervical ganglia is not surprising as these autonomic ganglia receive sensory input from CGRP-positive axons of trigeminal (25–27) and upper cervical ganglia, respectively. This presence identifies a need to investigate further the possibility that CGRP-mAbs may prevent certain aspects of a migraine attack by blocking CGRP-dependent interactions between sensory and autonomic functions (28) that help regulate the balance between parasympathetic and sympathetic tone in the cranium. Collectively, these findings provide strong support to the view that the prevention of migraine by CGRP-mAbs is attributable to their ability to block CGRP-dependent functions outside the brain (i.e. a direct action) that, in turn, alters multiple migraine-associated brain functions (i.e. an indirect action). This proposal raises two possibilities. The first is that the prolonged (years) and continuous bombardment of brain areas such as the spinal trigeminal nucleus, brainstem, thalamus, hypothalamus and cortex with pain signals that originate in the meninges renders them hypersensitive, hyper-responsiveness and hyper-excitable – to the extent that the smallest deviation from homeostasis can trigger an attack, the smallest exposure to light or sound can be aversive, and a relatively brief period of pain can give rise to central sensitization and allodynia. The second is that the elimination of pain signals that originate in the meninges, if maintained over time, allows spinal, brainstem, hypothalamic, thalamic and cortical neurons to regain a normal level of excitability and responsiveness seen in a non-migraine brain.

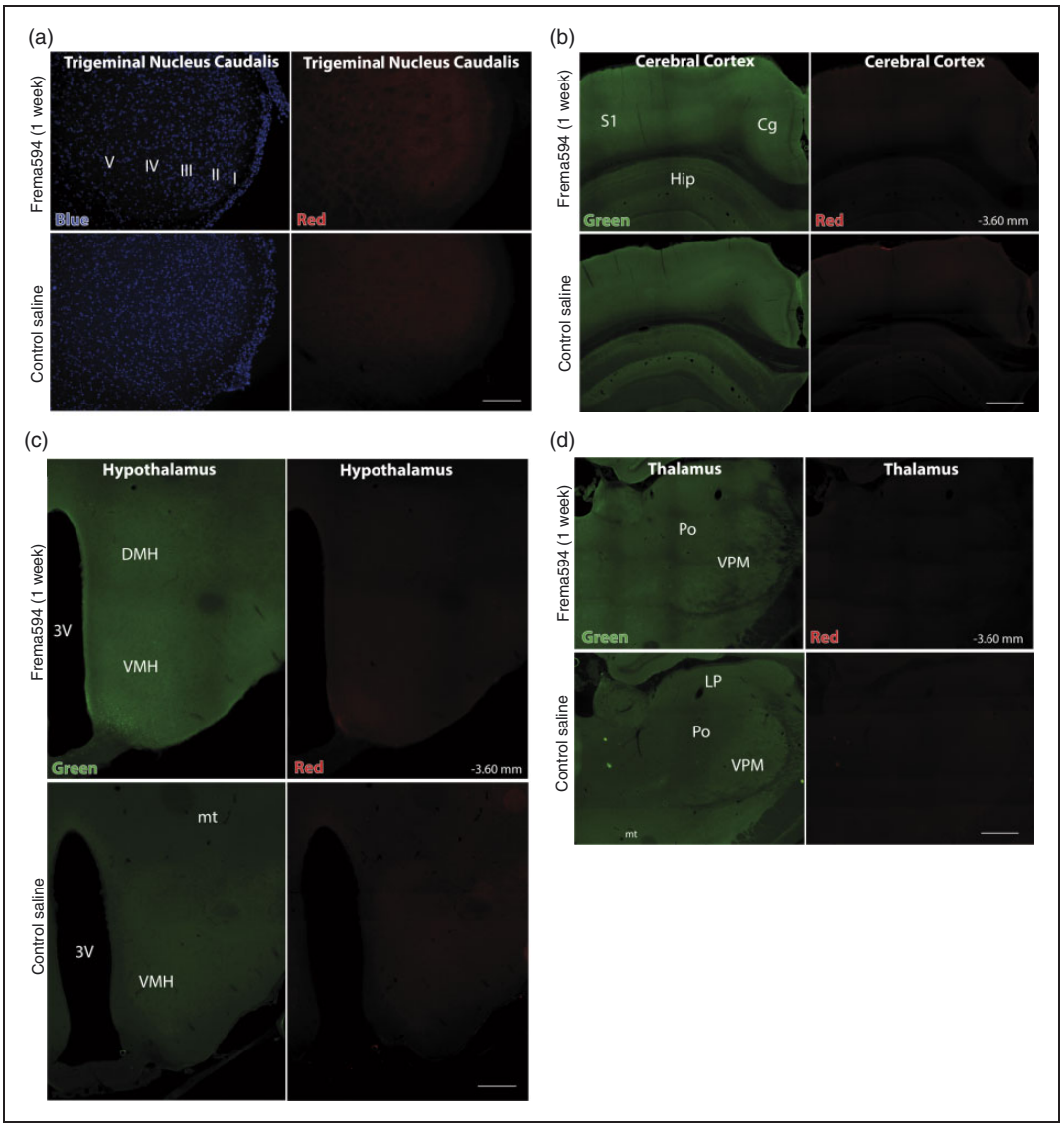

Figure 4. Fluorescent imaging of CNS structures (coronal view) in rats with un-compromised blood-brain barrier 1 week after i.v. injection of Frema594. Note that red positive Frema594 signal is not detected in coronal sections of the trigeminal nucleus caudalis (a), cerebral cortex (b), hypothalamus (c) or thalamus (d).
Cg: cingulate cortex; DMH: dorsomedial hypothalamus; Hip: hippocampus; LP: lateral-posterior thalamic nucleus; mt: mammillothalamic tract; Po: posterior thalamus; S1: primary somatosensory cortex; VMH: ventromedial hypothalamus; VPM: ventroposterior medial thalamic nucleus; 3 V: third ventricle. I-V: spinal cord dorsal horn laminae. Numbers in lower right indicate distance from *bregma*. Scale bar = 100 μm (a); 500 μm ((b)–(d)).

In rats in which the BBB was opened by the insertion of electrodes through the dura and pia into the cortex, fluorescent fremanezumab was clearly seen along the tract of the electrodes in the cortex, and in the pia surrounding the electrode penetration sites. We attribute the very limited passive diffusion of Frema594 (about 100 μm) to the fact that large molecules do not diffuse far in the brain (29,30). Surprisingly, most of the fremanezumab that was seen along the electrode tract in the cortex (at 4 hours after its injection) disappeared 1 week later. Its disappearance a week later raises the possibility that it was actively or passively cleared by the brain. Current evidence suggest that monoclonal antibodies can actively be cleared from the brain, within 24 hours, by the Fc receptor (31–33), or passively through bulk interstitial fluid flow through the glymphatic system to cervical lymph nodes (34–36). Another possible explanation for the absence of fremanezumab in the brain is that, by 1 week, the compromised BBB area in the dura was repaired/sealed by connective/scar tissue that grew over the electrode penetration sites, which would prevent further entry

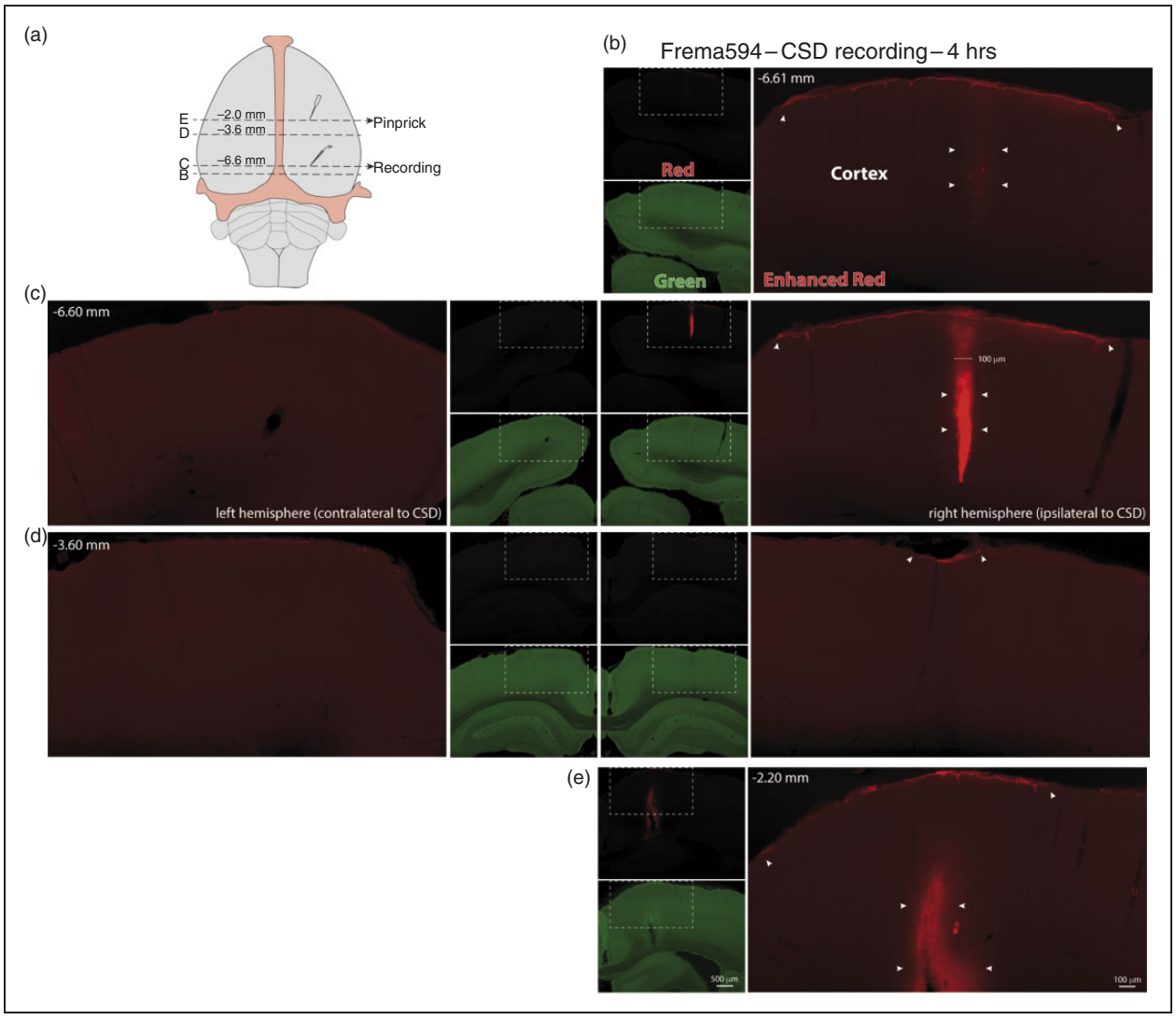

Figure 5. Fluorescent imaging of cerebral cortex (coronal view) in rats with *compromised* blood-brain barrier 4 hours after i.v. injection of Frema594. (a) Schematic overview of the rat brain depicting areas of images shown in B-E and locations of cortical disruptions. Numbers depict distance from bregma. (b) Minimal detection of Frema594 at 100 µm caudal to the electrode track and residual labeling in the overlying pia. (c) Accumulation of Frema594 along the track of the glass electrode used to record cortical spreading depression. Arrowheads depict limits of Frema594 spread. Note that in the cortex, Frema594 did not spread farther than 100 µm from the electrode track and that in the pia it spreads about 1 mm from the penetration site. Small images in red were acquired at default exposure. Small images in green and large images in red were overexposed post-acquisition for reference and visualization of anatomical structures.

of labeled fremanezumab. These observations may have further implications to the ongoing attempt to understand whether CGRP-mAbs enter the brain and if so, whether they are capable of altering any brain activity that can lead to a migraine attack for an extended (30 days) period.

Prior to the current study, three studies have evaluated BBB penetration of CGRP pathway modulators (two assessed penetration of small molecule CGRP receptor antagonists and one assessed the penetration of a CGRP-mAb). In the first, Vermeersch and colleagues (37) used the CGRP receptor positron emission tomography tracer [^{11}C]MK-4233 to quantify brain receptor occupancy in the ictal and interictal phases and found no evidence for enhanced occupancy after administration of telcagepant. They concluded that the BBB remains intact during a migraine attack. In the second, Hostetler and colleagues (38) used the same assay ([^{11}C]MK-4233} to quantify receptor occupancy in brains of rhesus monkeys and humans following intravenous injections of telcagepant. They found that at a clinically effective dose, no evidence for

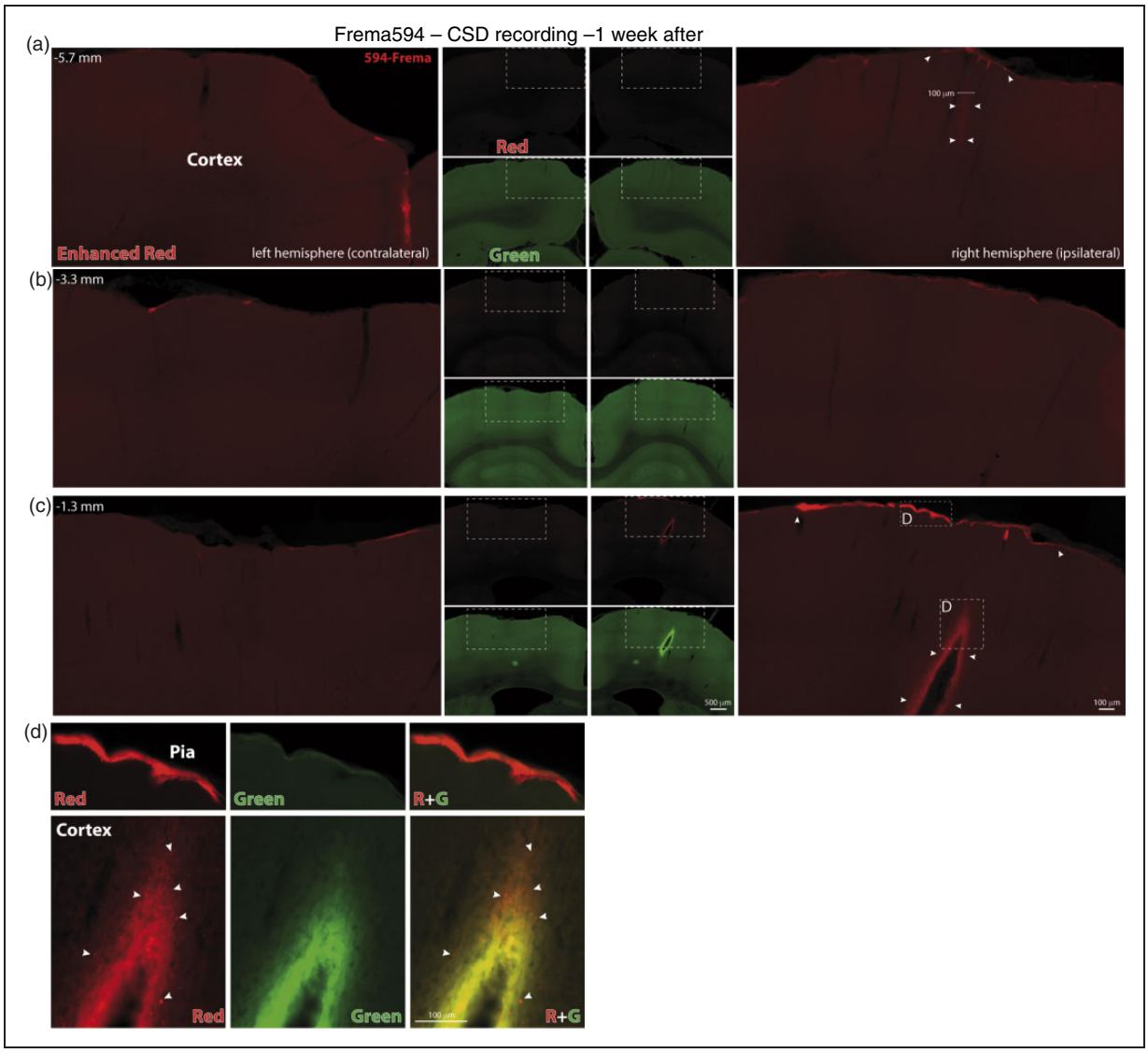

Figure 6. Fluorescent imaging of cerebral cortex (coronal view) in rats with *compromised* blood-brain barrier 1 week after i.v. injection of Frema594. (a) Cerebral cortex near the penetration of the recording electrode. Note that a positive red signal is barely detected (arrowheads). (b) Fluorescent images of the cortex at least 2 mm away from the recording electrode or CSD-induction electrode. (c) Fluorescent images of the cortex near the CSD-induction electrode. Note distinct Frema594 labeling in the pia (arrowheads), along the track of the CSD-induction electrode but not along the track of the recording electrode in (a). (d) High magnification images of the areas framed in (c) (right column), showing red and green channels and a superimposition of both images. Note that the pia is visible in red but not green channel images, confirming Frema594 presence in the pia of rats with compromised BBB. Also note that in the cortex, there are axons (arrowheads) that are labeled in red but not green channel images, raising the possibility that fremanezumab may be able to enter broken axons near a brain lesion. Signal in the green channel (middle) represents auto-fluorescence that is typical to formation of post-lesion gliosis. Small images in red were acquired at default exposure. Small images in green and large images in red (right and left columns) are overexposed for reference and visualization of anatomical structures. Dotted rectangles in small images depict enlarged images shown in red.

receptor occupancy was found in the brain – a finding that led Hargreaves and Olesen to conclude that the clinical effectiveness of telcagepant is achieved through its action outside the brain (39). In the third study, Johnson and colleagues (40) used radiolabeled galcanezumab ([125I] galcanezumab) and gamma counting techniques to evaluate the level of galcanezumab in peripheral and central tissues. They found high levels of galcanezumab in the dura and trigeminal ganglion and a very low level in the hypothalamus, spinal cord, cortex and cerebellum. Surprisingly, they found that the level of galcanezumab was almost equal in the

spinal cord or cortex (where the BBB is tight) and the hypothalamus, a brain area in which the BBB is largely compromised due to its anatomical and functional relationship with the portal system and the pituitary gland. It is surprising because it suggests that the higher penetrability of the BBB in the hypothalamus does not alter brain accessibility of these molecules.

Despite the difficulties in accurately detecting levels of CGRP-mAbs or receptor antagonists in the brain, the effort to determine if a central site of action can account for the clinical efficacy of CGRP modulators is scientifically justified. To do so, we must determine (a) whether CGRP receptors are found on hypothalamic neurons whose activity regulates different circadian rhythms, thalamic neurons that convey sensory information to the cortex, cortical neurons that set excitability tone, brainstem neurons that regulate pain transmission and many other neurons whose functional behavior can actually lead to a migraine attack; (b) whether CGRP can alter their activity in a way that can lead to prodromes, aura, hyperresponsiveness, sensitization, migraine attacks, headache, or distinct migraine-associated symptoms; (c) what causes CGRP to be released in these areas; (d) where is it released from; and most importantly (e) whether CGRP modulators reach these neurons at high enough concentrations to actually prevent CGRP from altering their behavior.

And finally, we must ask ourselves whether we really want to develop CGRP modulators that cross the BBB and reach all or most brain areas containing CGRP receptors. Presence of CGRP receptors in the amygdala (41–44), basal ganglia (41,43–46), hippocampus (11,44–47), septum (11,44–47), thalamus (11,43–45), hypothalamus (11,42–47), periaqueductal gray (33,42,43,45,47), and cerebellum (11,41,42,44,45) raises the possibility that central CGRP modulation may alter the many ways by which different neuronal circuits regulate sensory, motor, autonomic, endocrine, cognitive and affective functions. Would the gain of blocking CGRP signaling in the brain (potentially improved efficacy) outweigh the loss (potential introduction of multiple unwanted side effects)?

Key findings

- When the BBB is intact, intravenous administration of fluorescently labeled fremanezumab produces intense labeling of the monoclonal antibody in sensory and autonomic ganglia and in the dura, but not in any brain area or the pia.
- When the BBB is compromised, fremanezumab reaches the pia and brain areas in the vicinity of the broken BBB.
- Following local BBB disruption, brain clearance of fremanezumab is completed within a week.

Declaration of conflicting interests

The authors declared the following potential conflicts of interest with respect to the research, authorship, and/or publication of this article: Related to the current study, Rami Burstein received grant support for this study from Teva. He is also a consultant to Teva. Jennifer Stratton and Jason Tien are employees of Teva. Unrelated to the current study, Rami Burstein received grant support from Allergan, Dr. Reddy, Ely Lilly, and Trigemina. He is a consultant to Alder, Allergan, Amgen, Biohaven, Dr. Reddy, Electrocore, Johnson & Johnson, Neuroief, Percept, Teva, Theranica, and Trigemina. He is a member of the Scientific Advisory Board for Allergan, Ely Lilly, Teva, Dr. Reddy, Percept, and Trigemina.

Funding

The authors disclosed receipt of the following financial support for the research, authorship, and/or publication of this article: This study was supported by a grant from Teva (R.B.) and NIH grants R37-NS079678, R01-NS094198, R01-NS095655 (R.B.), R01 NS104296 (R.N.).

References

1. Hansen JM, Hauge AW, Olesen J, et al. Calcitonin gene-related peptide triggers migraine-like attacks in patients with migraine with aura. *Cephalalgia* 2010; 30: 1179–1186.
2. Goadsby PJ, Edvinsson L and Ekman R. Vasoactive peptide release in the extracerebral circulation of humans during migraine headache. *Ann Neurol* 1990; 28: 183–187.
3. Uddman R, Edvinsson L, Ekman R, et al. Innervation of the feline cerebral vasculature by nerve fibers containing calcitonin gene-related peptide: Trigeminal origin and co-existence with substance P. *Neurosci Lett* 1985; 62: 131–136.
4. Edvinsson L, Ekman R, Jansen I, et al. Peptide-containing nerve fibers in human cerebral arteries: Immunocytochemistry, radioimmunoassay, and in vitro pharmacology. *Ann Neurol* 1987; 21: 431–437.
5. Mason BN, Kaiser EA, Kuburas A, et al. Induction of migraine-like photophobic behavior in mice by both peripheral and central CGRP mechanisms. *J Neurosci* 2017; 37: 204–216.

6. Eftekhari S, Salvatore CA, Gaspar RC, et al. Localization of CGRP receptor components, CGRP, and receptor binding sites in human and rhesus cerebellar cortex. *Cerebellum* 2013; 12: 937–949.
7. Eftekhari S, Warfvinge K, Blixt FW, et al. Differentiation of nerve fibers storing CGRP and CGRP receptors in the peripheral trigeminovascular system. *J Pain* 2013; 14: 1289–1303.
8. Cottrell GS, Roosterman D, Marvizon JC, et al. Localization of calcitonin receptor-like receptor and receptor activity modifying protein 1 in enteric neurons, dorsal root ganglia, and the spinal cord of the rat. *J Comp Neurol* 2005; 490: 239–255.
9. Sugimoto T, Fujiyoshi Y, Xiao C, et al. Central projection of calcitonin gene-related peptide (CGRP)- and substance P (SP)-immunoreactive trigeminal primary neurons in the rat. *J Comp Neurol* 1997; 378: 425–442.
10. Hendrikse ER, Bower RL, Hay DL, et al. Molecular studies of CGRP and the CGRP family of peptides in the central nervous system. *Cephalalgia* 2019; 39: 403–419.
11. Warfvinge K and Edvinsson L. Distribution of CGRP and CGRP receptor components in the rat brain. *Cephalalgia* 2019; 39: 342–353.
12. Edvinsson L, Fredholm BB, Hamel E, et al. Perivascular peptides relax cerebral arteries concomitant with stimulation of cyclic adenosine monophosphate accumulation or release of an endothelium-derived relaxing factor in the cat. *Neurosci Lett* 1985; 58: 213–217.
13. Burstein R, Noseda R and Borsook D. Migraine: multiple processes, complex pathophysiology. *J Neurosci* 2015; 35: 6619–6629.
14. Silberstein SD, Dodick DW, Bigal ME, et al. Fremanezumab for the preventive treatment of chronic migraine. *N Engl J Med* 2017; 377: 2113–2122.
15. Goadsby PJ, Reuter U, Hallstrom Y, et al. A controlled trial of erenumab for episodic migraine. *N Engl J Med* 2017; 377: 2123–2132.
16. Dodick DW, Goadsby PJ, Silberstein SD, et al. Safety and efficacy of ALD403, an antibody to calcitonin gene-related peptide, for the prevention of frequent episodic migraine: A randomised, double-blind, placebo-controlled, exploratory phase 2 trial. *Lancet Neurol* 2014; 13: 1100–1107.
17. Dodick DW, Goadsby PJ, Spierings EL, et al. Safety and efficacy of LY2951742, a monoclonal antibody to calcitonin gene-related peptide, for the prevention of migraine: A phase 2, randomised, double-blind, placebo-controlled study. *Lancet Neurol* 2014; 13: 885–892.
18. Melo-Carrillo A, Strassman AM, Nir RR, et al. Fremanezumab-A humanized monoclonal anti-CGRP antibody inhibits thinly myelinated (Adelta) but not unmyelinated (C) meningeal nociceptors. *J Neurosci* 2017; 37: 10587–10596.
19. Melo-Carrillo A, Noseda R, Nir RR, et al. Selective inhibition of trigeminovascular neurons by fremanezumab: A humanized monoclonal anti-CGRP antibody. *J Neurosci* 2017; 37: 7149–7163.
20. Schain AJ, Melo-Carrillo A, Stratton J, et al. CSD-induced arterial dilatation and plasma protein extravasation are unaffected by fremanezumab: Implications for CGRP's role in migraine with aura. *J Neurosci* 2019; 39: 6001–6011.
21. Ten Tusscher MP, Klooster J and Vrensen GF. Satellite cells as blood-ganglion cell barrier in autonomic ganglia. *Brain Res* 1989; 490: 95–102.
22. Allen DT and Kiernan JA. Permeation of proteins from the blood into peripheral nerves and ganglia. *Neuroscience* 1994; 59: 755–764.
23. Eftekhari S, Salvatore CA, Calamari A, et al. Differential distribution of calcitonin gene-related peptide and its receptor components in the human trigeminal ganglion. *Neuroscience* 2010; 169: 683–696.
24. Eftekhari S and Edvinsson L. Possible sites of action of the new calcitonin gene-related peptide receptor antagonists. *Ther Adv Neurol Disord* 2010; 3: 369–378.
25. Ivanusic JJ, Kwok MMK, Ahn AH, et al. 5-HT(1D) receptor immunoreactivity in the sphenopalatine ganglion: Implications for the efficacy of triptans in the treatment of autonomic signs associated with cluster headache. *Headache* 2011; 51: 392–402.
26. Zaidi ZF and Matthews MR. Source and origin of nerve fibres immunoreactive for substance P and calcitonin gene-related peptide in the normal and chronically denervated superior cervical sympathetic ganglion of the rat. *Auton Neurosci* 2013; 173: 28–38.
27. Yamamoto K, Senba E, Matsunaga T, et al. Calcitonin gene-related peptide containing sympathetic preganglionic and sensory neurons projecting to the superior cervical ganglion of the rat. *Brain Res* 1989; 487: 158–164.
28. Csati A, Tajti J, Tuka B, et al. Calcitonin gene-related peptide and its receptor components in the human sphenopalatine ganglion – interaction with the sensory system. *Brain Res* 2012; 1435: 29–39.
29. Hopkins K, Chandler C, Eatough J, et al. Direct injection of 90Y MoAbs into glioma tumor resection cavities leads to limited diffusion of the radioimmunoconjugates into normal brain parenchyma: A model to estimate absorbed radiation dose. *Int J Radiat Oncol Biol Phys* 1998; 40: 835–844.
30. Salvatore MF, Ai Y, Fischer B, et al. Point source concentration of GDNF may explain failure of phase II clinical trial. *Exp Neurol* 2006; 202: 497–505.
31. Cooper PR, Ciambrone GJ, Kliwinski CM, et al. Efflux of monoclonal antibodies from rat brain by neonatal Fc receptor, FcRn. *Brain Res* 2013; 1534: 13–21.
32. Deane R, Sagare A, Hamm K, et al. IgG-assisted age-dependent clearance of Alzheimer's amyloid beta peptide by the blood-brain barrier neonatal Fc receptor. *J Neurosci* 2005; 25: 11495–11503.
33. Zhang Y and Pardridge WM. Mediated efflux of IgG molecules from brain to blood across the blood-brain barrier. *J Neuroimmunol* 2001; 114: 168–172.
34. Weller RO, Djuanda E, Yow HY, et al. Lymphatic drainage of the brain and the pathophysiology of neurological disease. *Acta Neuropathol* 2009; 117: 1–14.

35. Koh L, Zakharov A and Johnston M. Integration of the subarachnoid space and lymphatics: Is it time to embrace a new concept of cerebrospinal fluid absorption? *Cerebrospinal Fluid Res* 2005; 2: 6.
36. Aspelund A, Antila S, Proulx ST, et al. A dural lymphatic vascular system that drains brain interstitial fluid and macromolecules. *J Exp Med* 2015; 212: 991–999.
37. Vermeersch S, De Hoon JN, De Saint-Hubert B, et al. PET imaging in healthy subjects and migraineurs suggests CGRP receptor antagonists do not have to act centrally to achieve clinical efficacy. *J Headache Pain* 2013; 14(Suppl 1): 224.
38. Hostetler ED, Joshi AD, Sanabria-Bohorquez S, et al. In vivo quantification of calcitonin gene-related peptide receptor occupancy by telcagepant in rhesus monkey and human brain using the positron emission tomography tracer [11C]MK-4232. *J Pharmacol Exp Ther* 2013; 347: 478–486.
39. Hargreaves R and Olesen J. Calcitonin gene-related peptide modulators - the history and renaissance of a new migraine drug class. *Headache* 2019; 59: 951–970.
40. Johnson KW, Morin SM, Wroblewski VJ, et al. Peripheral and central nervous system distribution of the CGRP neutralizing antibody [(125)I] galcanezumab in male rats. *Cephalalgia* 2019; 39: 1241–1248.
41. Becskei C, Riediger T, Zund D, et al. Immunohistochemical mapping of calcitonin receptors in the adult rat brain. *Brain Res* 2004; 1030: 221–233.
42. Olgiati VR, Guidobono F, Netti C, et al. Localization of calcitonin binding sites in rat central nervous system: Evidence of its neuroactivity. *Brain Res* 1983; 265: 209–215.
43. Kresse A, Jacobowitz DM and Skofitsch G. Detailed mapping of CGRP mRNA expression in the rat central nervous system: Comparison with previous immunocytochemical findings. *Brain Res Bull* 1995; 36: 261–274.
44. Stachniak TJ and Krukoff TL. Receptor activity modifying protein 2 distribution in the rat central nervous system and regulation by changes in blood pressure. *J Neuroendocrinol* 2003; 15: 840–850.
45. Oliver KR, Kane SA, Salvatore CA, et al. Cloning, characterization and central nervous system distribution of receptor activity modifying proteins in the rat. *Eur J Neurosci* 2001; 14: 618–628.
46. Tolcos M, Tikellis C, Rees S, et al. Ontogeny of calcitonin receptor mRNA and protein in the developing central nervous system of the rat. *J Comp Neurol* 2003; 456: 29–38.
47. Sexton PM, Paxinos G, Kenney MA, et al. In vitro autoradiographic localization of amylin binding sites in rat brain. *Neuroscience* 1994; 62: 553–567.